http://dx.doi.org/10.5012/bkcs.2013.34.1.99

Electrical Conductivity, Dielectric Behavior and EMI Shielding Effectiveness of Polyaniline-Yttrium Oxide Composites

Muhammad Faisal[†] and Syed Khasim[†,‡,*]

[†]*Department of Physics, PES Institute of Technology-Bangalore South Campus, Bangalore-560 100, Karnataka, India*
[‡]*Department of Physics, University of Tabuk-71491, Kingdom of Saudi Arabia.* [*]*E-mail: syed.pes@gmail.com*
Received July 20, 2012, Accepted October 12, 2012

Polyaniline-yttrium trioxide (PAni-Y_2O_3) composites were synthesized by the *in-situ* polymerization of aniline in the presence of Y_2O_3. The composite formation and structural changes in these composites were investigated by X-ray diffraction (XRD), Fourier transform infra red spectroscopy (FTIR), scanning electron microscopy (SEM) and high resolution transmission electron microscopy (HRTEM). The direct current (DC) electrical conductivity of the order of 0.51×10^{-2} S cm^{-1} - 0.283 S cm^{-1} in the temperature range 300 K-473 K indicates semiconducting behavior of the composites. Room temperature AC conductivity and dielectric response of the composites were studied in the frequency range of 10 Hz to 1 MHz. The variation of AC conductivity with frequency obeyed the power law, which decreased with increasing weight percentage (wt %) of Y_2O_3. Studies on dielectric properties shows the relaxation contribution coupled by electrode polarization effect. The dielectric constant and dielectric loss in these composites depend on the content of Y_2O_3 with a percolation threshold at 20 wt % of Y_2O_3 in PAni. Electromagnetic interference shielding effectiveness (EMI SE) of the composites in the frequency range 100 Hz to 2 GHz was in the practically useful range of –12.2 dB to –17.2 dB. The observed electrical and shielding properties were attributed to the interaction of Y_2O_3 particles with the PAni molecular chains.

Key Words : Polyaniline composites, Conductivity, EMI shielding, Yttrium trioxide

Introduction

Conducting polymers have been an area of immense interest over the past few decades owing to the growing technological applications in rechargeable batteries, EMI shielding, microelectronics, sensors, electrochromic displays, photovoltaic devices, *etc.*[1,2] Among the various conducting polymers, polyaniline (PAni) has received special attention because of its easy preparation, environmental stability, interesting redox behavior and tunable electrical, optical properties.[3-6] The electrical properties of conducting polymer could be modified by the addition of inorganic fillers.[7-10] A tunable electrical conductivity was reported for PAni-TiO_2 composite.[11] Also, a dielectric constant as high as 3700 has been observed for PAni-TiO_2 nanocomposites.[7] Composites of PAni with dispersant TiO_2 have been widely studied by employing various techniques towards synthesis and characterization with modifications in different properties.[12-15] Conducting polymer-inorganic oxide composites are expected to improve or complement the electrical, electromagnetic, chemical and structural properties over their single components, to achieve maximum efficiency required on the different processes taking place in specific applications.[16-21] It is important to analyze the transport and electromagnetic properties of these composites to identify the influence of dispersant on the properties of the conducting polymer matrix.[22] These composites are considered as heterogeneous disordered systems with a complementary behavior between the two.[23] The properties of these new functional materials depends on a number of factors such as concentration of the dispersant, their morphology, orientation and interfacial interaction with the matrix.[24] Such conducting polymer based composites are expected to exhibit EMI shielding and electrostatic dissipation of charges (ESD) due to their modified electrical and dielectric properties.[25] Most of the conducting polymer composite systems studied in the literature refer to their physical characteristics and mechanism of electric transport,[4-16,19,20,22] but the studies on EMI shielding properties in the low frequency range are very limited.

The EMI shielding has become a growing concern in the recent past to protect the equipments from electromagnetic hazards. Thus the study of materials that can prevent electromagnetic interference (EMI) has greater relevance. Electrical conductivity is a prerequisite for a shielding material, and how best the material shields the electromagnetic radiation is analyzed as electromagnetic interference shielding effectiveness (EMI SE).[26]

The present study is focused on the electrical and EMI shielding behavior of PAni-Y_2O_3 composites. In this work we have tried to bring out structure property correlation with a comparison between electric transport and EMI shielding studies in low frequency range for PAni-Y_2O_3 composites. To the best of our knowledge no study has been reported on the low frequency (100 Hz-2 GHz) EMI shielding behavior of PAni-Y_2O_3 composites. Y_2O_3 is an excellent host for rare earth ions and facilitates excellent microwave and dielectric properties.[27,28] Y_2O_3 has good thermal stability up to 2200 °C with high dielectric constant and only small deviations from

stoichiometry under normal conditions of temperature and pressure.[29] The effect of Y_2O_3 concentration on the DC electrical conductivity of the composites was analyzed in the temperature range from 300 K to 473 K. The frequency dependent dielectric constant and the conductivity were investigated in the low frequency range from 10 Hz to 1 MHz. The EMI shielding effectiveness of the composites was measured in the frequency range 100 Hz-2 GHz.

Experimental

Synthesis and Processing of PAni-Y_2O_3 Composites. All the chemicals used were of research grade. The monomer aniline (Sigma-Aldrich, India) was doubly distilled before use. Deionized and distilled water was used to prepare all the aqueous solutions. The chemical oxidative polymerization of monomer aniline was carried out in the presence of fine graded Y_2O_3 particles (Sigma-Aldrich, India) in acidic medium with ammonium persulphate (APS) as oxidant.[30] 1 M hydrochloric acid (HCl) and Y_2O_3 were homogenized by vigorous stirring for 1 h. To this 0.5 M of aniline was added and vigorous stirring was continued for 1 h to form an emulsion. The oxidant APS was added drop-by-drop keeping the temperature of the reaction mixture at 0-5 °C with vigorous stirring for 6 h to the above emulsion. The resultant solution was filtered and washed thoroughly with water and acetone and dried at 50 °C in a vacuum oven. Thus different composition of the PAni-Y_2O_3 composites with different weight percentage of Y_2O_3 in PAni (PYO1 - PAni with 10 wt % of Y_2O_3, PYO2 - PAni with 20 wt % of Y_2O_3, PYO3 - PAni with 30 wt % of Y_2O_3, PYO4 - PAni with 40 wt % of Y_2O_3 and PYO5 - PAni with 50 wt % of Y_2O_3) were synthesized to check the effect of Y_2O_3 dispersant in the PAni matrix.

The synthesized PAni-Y_2O_3 composites were compacted into circular pellets for the electrical conductivity studies. Pellets of 10 mm diameter and 2-2.5 mm thickness were made at room temperature using a homemade die under a pressure of 9 tons in a table top hydraulic press. Similarly, the composites were prepared in rectangular pellet form for the measurement of EMI shielding effectiveness. The quantity of the composite sample, applied pressure and pressing time were optimized and maintained for both the circular and rectangular pellet samples.

Measurements

X-ray powder diffraction studies were carried out at ambient temperature using a Rigaku X-ray diffractometer (model: RU-300, Japan) with Cu-Kα (1.54 Å) radiation. The patterns were recorded in a wide range of 3-80° at 0.02° step size. Infrared spectra of the samples were recorded using a PerkinElmer FTIR spectrophotometer (model: 783, USA) in KBr medium. A Philips SEM (model - XL30 ESEM, Netherlands) was employed to study the surface morphology of PAni, Y_2O_3 and PAni-Y_2O_3 composites. HRTEM was carried out on JOEL JEM 2100 (Japan) with point resolution of 1.44 Å and line resolution of 2.32 Å.

Temperature dependent DC conductivity of the composites were performed by two-probe technique using a laboratory made setup with Keithley 224 constant current source and Keithley 617 digital electrometer. The measurements were recorded during cooling cycle. AC conductivity and dielectric measurements were carried out at room temperature over the frequency range 100 Hz-1 MHz, using Hioki LCR meter (model: 3532-50, Japan). The rectangular pellets were used for the EMI shielding effectiveness measurement by transmission line technique[31] in an Advantest spectrum analyzer (model: R4131D, Japan) in the frequency range from 100 Hz to 2 GHz.

Results and Discussion

X-ray Diffraction Analysis. The XRD patterns of polyaniline, Y_2O_3 and PAni-Y_2O_3 composite are shown in Figure 1 (a, b and c). The XRD pattern of polyaniline (Fig. 1(a)) shows amorphous features with broad semicrystalline diffraction peaks centered at around 2θ = 21° and 28°. These peaks correspond to the scattering from bare polymer chains of the protonated polyaniline.[30,32] It has been reported that the structure of polyaniline doped with common counter ions are predominately amorphous.[3] Figure 1(b) shows the diffraction peaks corresponding to single phase of cubic Y_2O_3 (JCPDS 41-1105). For PAni-Y_2O_3 composite (Fig. 1(c)), the diffraction peaks of Y_2O_3 can be clearly observed in the composite, with a slight variation of intensity. This confirms that Y_2O_3 retained its structure even after the formation of composite.

FTIR Analysis. The FTIR spectra recorded for polyaniline, Y_2O_3 and PAni-Y_2O_3 composite are as shown in Figure 2 (a, b, and c). In Figure 2(a), the characteristic peaks of pure PAni observed around 1568, 1484, 1299, 1243, 1120 and 809 cm^{-1}. The absorption peaks at 1568 and 1484 cm^{-1} are assigned to the C=C bond stretching of the quinoid and benzenoid rings.[33] The peaks at 1299 and 1243 cm^{-1} are attributed to the C–N stretching modes of the benzenoid

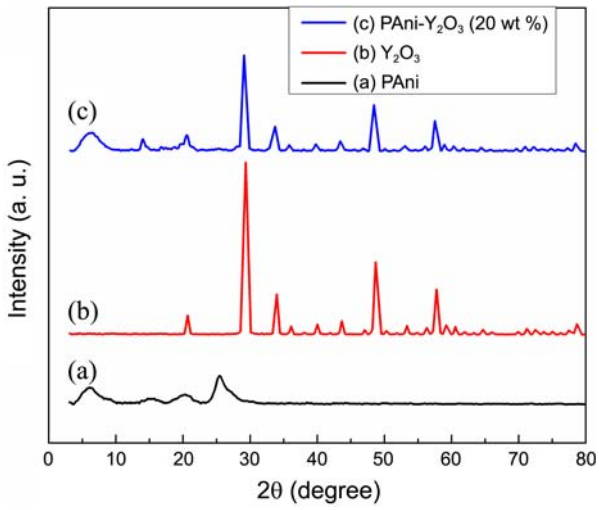

Figure 1. XRD spectra of: (a) PAni, (b) Y_2O_3, and (c) PAni-Y_2O_3 composite (20 wt %).

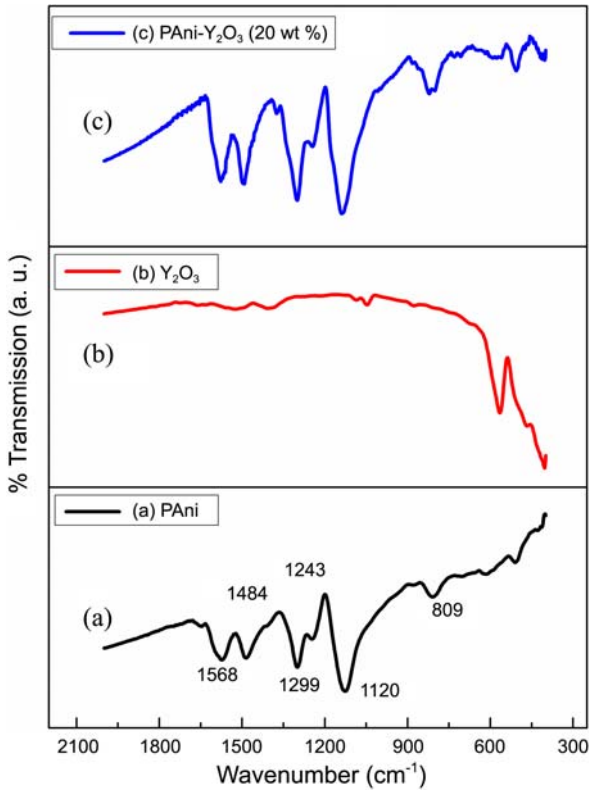

Figure 2. FTIR spectra of: (a) PAni, (b) Y_2O_3, and (c) PAni-Y_2O_3 composite (20 wt %).

rings. The peak at 1120 cm^{-1} is assigned to an in-plane bending vibration of the C–H bonds formed during the protonation.[34,35] The peak at 809 cm^{-1} is attributed to the out of plane deformation of C–H in the p-disubstituted benzene ring.[35,36] The FTIR spectrum for Y_2O_3 shown in Figure 2(b), the high intensity peaks centered around 600 cm^{-1} attributed to Y–O stretching mode of Y_2O_3 structure. From the Figure 2(c), it is observed that the characteristic peaks of pure PAni are very well reflected in PAni-Y_2O_3 composite with small shift, indicating the effect of Y_2O_3 addition in PAni. The introduction of Y_2O_3 altered the conjugated backbone structure of PAni. The corresponding peaks of pure PAni at 1568 cm^{-1} shifted to 1577 cm^{-1}, 1484 cm^{-1} shifted to 1492 cm^{-1}, 1299 cm^{-1} shifted to 1300 cm^{-1}, 1243 cm^{-1} shifted to 1246 cm^{-1}, 1120 cm^{-1} shifted to 1138 cm^{-1} and 809 cm^{-1} shifted to 821 cm^{-1} wavenumbers in PAni-Y_2O_3 (20 wt %) composite. These shifts clearly indicate the vanderwaal's type of interaction between PAni and Y_2O_3 during the composite formation.

SEM Studies. The SEM micrographs for PAni, Y_2O_3 and PAni-Y_2O_3 composites are shown in Figure 3 (a, b and c). The micrograph of pristine PAni shown in Figure 3(a) indicates the agglomerated globular structure.[33] The SEM image of Y_2O_3 (Fig. 3(b)) shows the presence of plate like structure for Y_2O_3 particles with random grain orientation. The Y_2O_3 particles exhibited agglomeration because of the dipole interaction. The composite shown in Figure 3(c) exhibit distinct morphology compared to that of pure PAni and bare Y_2O_3 particles. The polymerization of aniline over Y_2O_3 particles (for PAni-Y_2O_3 composite with 20 wt % of

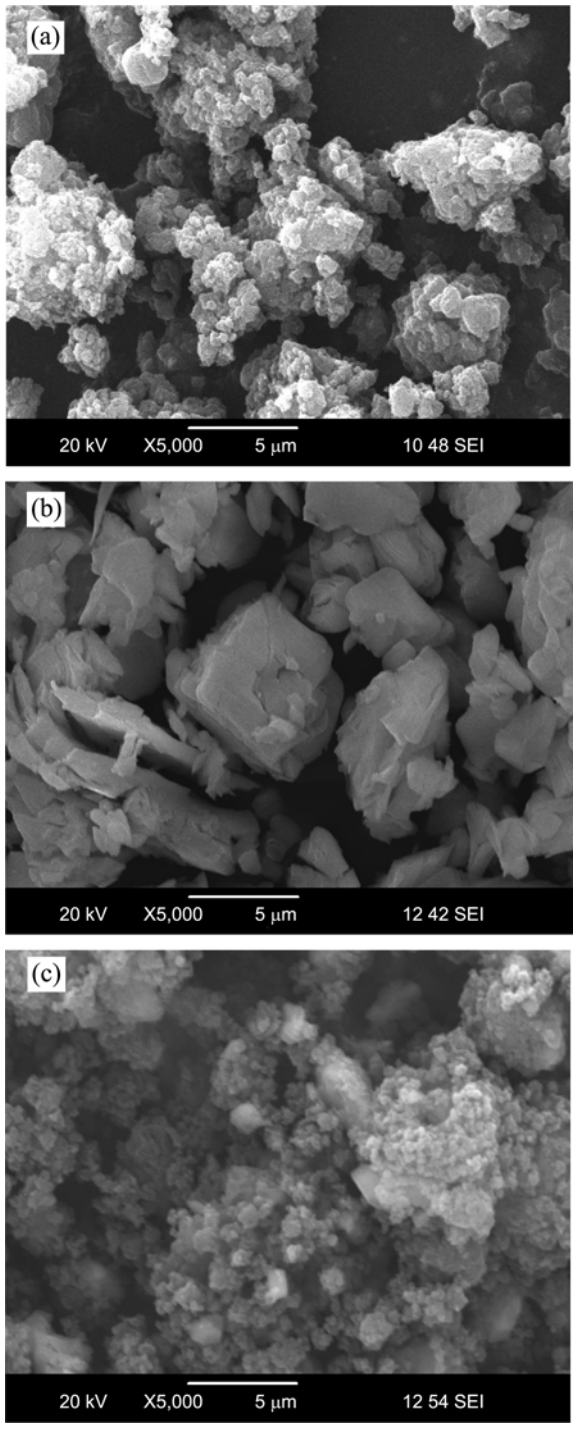

Figure 3. SEM photographs of: (a) PAni, (b) Y_2O_3 and (c) PAni-Y_2O_3 composite (20 wt %).

Y_2O_3 in PAni) is observed with globular agglomeration. The modification of morphology was distinct in the composites leading to various electrical and electromagnetic properties different from pristine PAni and Y_2O_3.

HRTEM Analysis. TEM images of Y_2O_3 and PAni-Y_2O_3 composite are shown in Figure 4 (a and b) whereas Figure 4(c) shows the high magnification HRTEM image of the PAni-Y_2O_3 composite. From Figure 4(a), the particle size of Y_2O_3 was estimated to be 100-130 nm. When these Y_2O_3

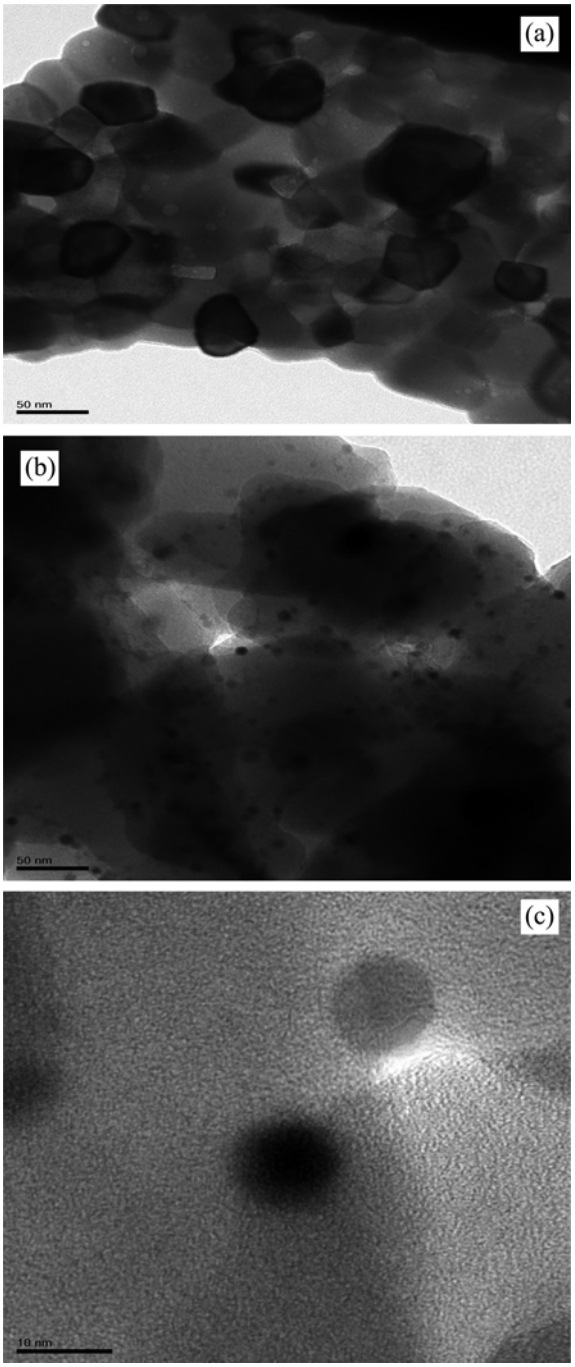

Figure 4. Low magnification HRTEM image of: (a) Y_2O_3, (b) PAni-Y_2O_3 composite; (c) high magnification HRTEM image of PAni-Y_2O_3 composite.

particles were incorporated in the PAni matrix, they show the agglomerated morphology (Fig. 4(b)). The homogeneous dispersion of Y_2O_3 particles in the polymer matrix is confirmed by the high magnification HRTEM image (Fig. 4(c)). In the composites, PAni matrix act as binder that distributes external load to the Y_2O_3 particles. In addition to increasing the rigidity of the polyaniline matrix, the particles are added to modify the rheological property. Thus conformational energy map of PAni macromolecules may display very rigid and extended structure and exhibit novel functionalities.

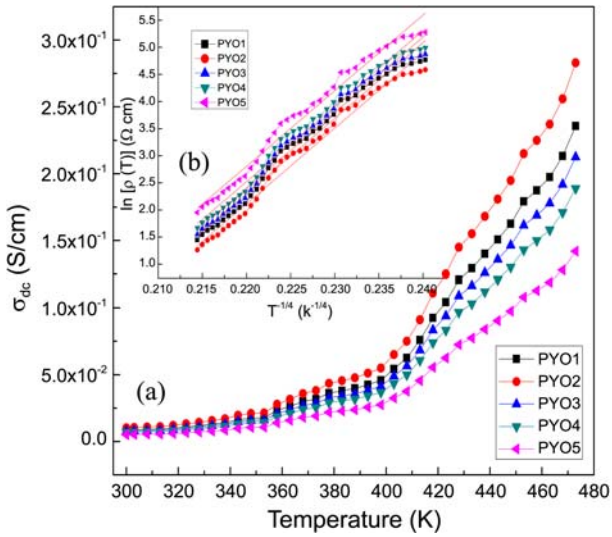

Figure 5. (a) Temperature dependent DC conductivity (σ_{dc}) of PAni-Y_2O_3 composites, (b) variation of DC resistivity of PAni-Y_2O_3 composites with temperature.

DC Conductivity. The temperature dependent DC conductivity (σ_{dc}) characteristics of PAni-Y_2O_3 composites are shown in Figure 5(a). The increase in DC conductivity of the composites was minimal in the low temperature region up to 353 K and increased thereafter steadily up to 473 K. The conductivity of all the composite samples (in the range 0.51×10^{-2} S cm^{-1} to 0.283 S cm^{-1}) increased with increasing temperature indicates typical semiconducting behavior. Similar observation was reported by Anilkumar *et al*.[38] Considering the effect of preparation methods, intrinsic properties such as molecular weight, morphology and crystallinity, and extrinsic properties such as the dopants, the conductivity of polyaniline varies between standard polymer (10^{-9} S cm^{-1}) and semiconductors (10^{0} S cm^{-1}) can be obtained.[39-41] Figure 5(b) shows the temperature variation of the resistivity ρ (T) of PAni-Y_2O_3 composites. The temperature dependence of resistivity for disordered semiconducting system is described in terms of variable range hopping model as[42,43]

$$\rho\,(T) = \rho_0 \exp\,(T_0/T)^{1/1+d} \qquad (1)$$

where, ρ_0 is a constant, d = 1, 2 and 3 is connected with the effective dimensionality of the charge transport in the semiconducting system and T_0 is the characteristic Mott temperature (slope of ln ρ(T) ~ $T^{-1/4}$ plot). Smaller value of T_0 indicates higher conductivity of the system. Thus the temperature dependence of resistivity [ρ(T)] of the PAni-Y_2O_3 composites follows ln ρ(T) ~ $T^{-1/4}$, described by variable range hopping model. A linear variation was observed in the graph of ln ρ(T) with $T^{-1/4}$ throughout the entire temperature range indicating the three-dimensional hopping transport property (Fig. 5(b)). That is, at higher temperatures hopping of charge carriers between localized states lead to increase in conductivity.[43] The DC conductivity increased for lower content of Y_2O_3 (10 and 20 wt %), which may be caused by the mobility of counterions of Y_2O_3 at higher temperature and decreases slightly with higher concent-

rations of Y_2O_3 (30, 40 and 50 wt %), due to the trapping of charge carriers (Fig. 5(a)).[44] The crowding of Y_2O_3 particles corresponding to higher concentrations hinders the path of charge carriers and partial blocking of charge carriers. Therefore these materials with moderate conductivity and morphological specialties can block incoming electromagnetic waves more effectively and can act as a shield for electromagnetic fields.

Low Frequency Transport Properties.

AC Conductivity: Low frequency AC conductivity of PAni-Y_2O_3 composites are represented in Figure 6(a). The frequency dependent conductivity in these composites varies in the range 10^{-3} to 10^{-1} (S cm^{-1}) is due to the semi crystalline nature of the PAni-Y_2O_3 composites as indicated by the X-ray diffractograms. The AC response of all the composites exhibits a frequency independent conductivity in the low frequency region up to 2 kHz and then increased as the frequency increased. This frequency independent plateau followed by a high frequency dispersed region in these composites obeyed the power law indicating the universal behavior of the ac conductivity in disordered media.[45-47] The empirical Jonscher's universal law $\sigma_{ac} \alpha \omega^n$,[47] where *n* is a fractional exponent roughly treated as constant less than 1, is often used to describe the ac component contributing to the dispersive region in the high frequency. This type of behavior is observed not only in conducting polyaniline composites but also in materials such as disordered polymers, semi conductors, heavily doped ionic crystals, ion conducting glasses *etc*.[23,47,48] Since the PAni-Y_2O_3 composite can be considered as a disordered system with a network of conduction paths of various lengths accessible to the charge carriers (polarons/bipolarons). Also the variation of conductivity with frequency dependent electric field is sensitive to sample preparation conditions and doping, as they influence the electric charge carrier (polaron/bipolaron) intra-chain/ inter-chain hopping. In the low frequency region the frequency independent macroscopic conductivity was considered to be completed through the charge flow along the conductive paths (or clusters) of the PAni-Y_2O_3 matrix and the paths connecting opposite surfaces of the composite sample where electrodes were attached. In the dispersive region, macroscopic conductivity was enhanced by the shorter length paths and the capacitive effects giving rise to polarization. The electrode polarization effects with the space charge polarization contributed the increase in conductivity of PAni-Y_2O_3 composites in the high frequency region. Similar AC conductivity behavior was reported by Jiang *et al*.[49] These electrical conductivity measurements are known to be very sensitive for the study of electronic properties of materials.

Figure 6(b) (inset) shows the variation of σ_{ac} as a function of wt % of dispersant Y_2O_3 in PAni at three selected frequencies (10 KHz, 100 KHz and 1000 KHz). Among the various compositions of PAni-Y_2O_3 composites, there was a slight increase in the conductivity observed up to 20 wt % loading of Y_2O_3, as observed in the case of DC electrical conductivity and thereafter a decrease for 30, 40 and 50 wt % concentrations of Y_2O_3. The lower concentrations of Y_2O_3 in Polyaniline matrix might have provided better connectivity for the conductive paths reflected in the increase of AC conductivity. The higher loadings of Y_2O_3 might have increased the disorderliness in the composites and hence a reduction in the delocalization length. This behavior is indicative of percolation character in PAni-Y_2O_3 composite systems, with percolation threshold at 20 wt % loading of Y_2O_3 in PAni.

Dielectric Properties. Figure 7 shows the variation of real part of dielectric constant (ε') with frequency (f). The obtained high values are related to the effects of electrode polarization and space charge polarization.[50] Dielectric constant of conducting polymer composite are dependent on composition, protonation, temperature and delocalization length.[51] It was observed that in all these composites, as frequency increased dielectric constant decreased sharply up

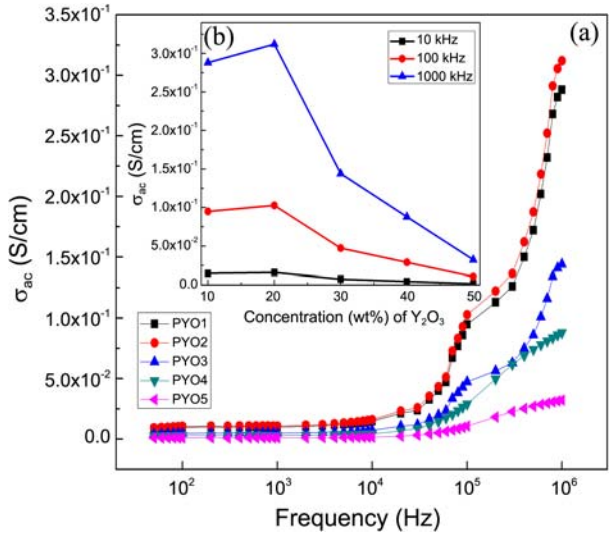

Figure 6. (a) Low frequency AC conductivity (σ_{ac}) of PAni-Y_2O_3 composites and (b) Variation of σ_{ac} as a function of wt % of Y_2O_3 in PAni.

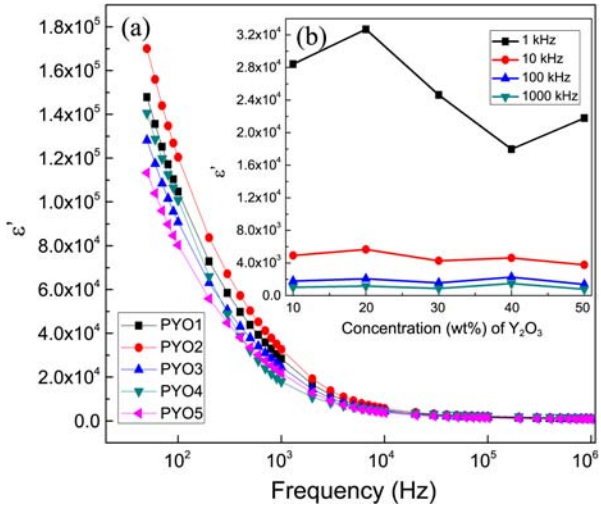

Figure 7. Variation of real part of dielectric constant (ε') of PAni-Y_2O_3 composites with frequency.

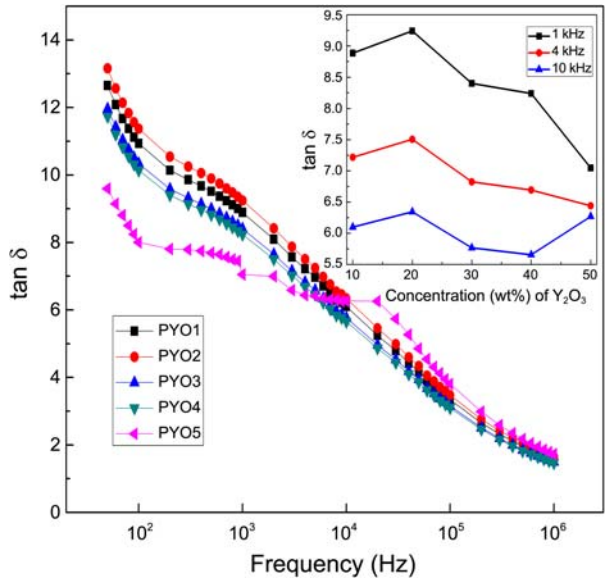

Figure 8. Variation of dissipation factor (tan δ) of PAni-Y_2O_3 composites with frequency.

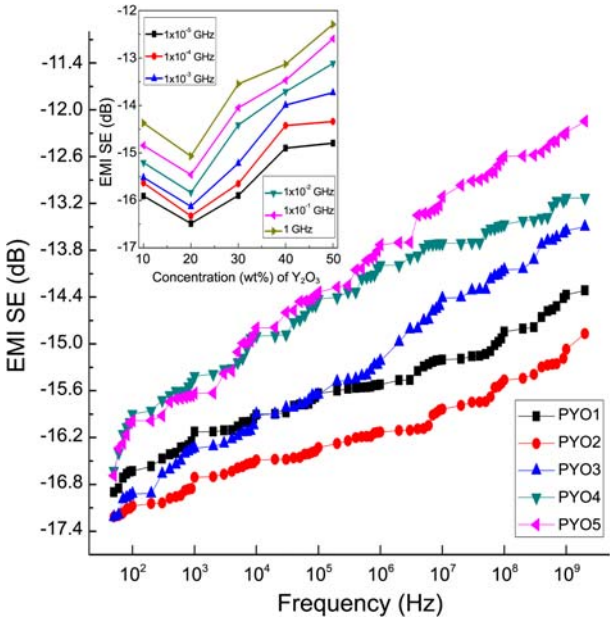

Figure 9. Low frequency (100 Hz to 2 GHz) EMI shielding effectiveness of PAni-Y_2O_3 composites.

to the frequency range of 10^3 and became constant at high frequencies. PAni is a semiconducting system with mobile polaron/bipolaron which is free to move along the chain where as the bound charges (dipoles) which have only restricted mobility resulting in strong polarization in the system. Thus upon increase in the frequency of the applied field, the dipoles present in the system cannot reorient themselves quickly in response to the applied field reducing the dielectric constant.

The dielectric constant shows an increase with increasing concentration of Y_2O_3 up to 20 wt % and decreased for higher concentrations 30, 40 and 50 wt % (as shown in inset). These results are in accordance with the observed conductivity behavior of PAni-Y_2O_3 composites. The strong frequency dispersion of permittivity of the PAni-Y_2O_3 composites was observed in the low frequency region, indicating the influence of relative dielectric constant of PAni and Y_2O_3. The decrease of ε' with frequency may be attributed to the electrical relaxation processes. But these relaxation process, do not merely come from extrinsic effects due to interfacial polarization from the electrode/sample interface, they also have an intrinsic origin in the bulk composite material.[52]

Figure 8 shows the variation of the dissipation factor, tan δ, recorded as a function of frequency for PAni-Y_2O_3 composites. It is observed that the dielectric loss decreases as a function of frequency. Conducting polymers and their composites maintains a balanced dielectric loss with variations sensitive to the dispersed phase. PAni-Y_2O_3 composites exhibited small values of tan δ in the frequency region around 1 MHz. As the loading of Y_2O_3 enhances the conductivity of the composites up to a concentration of 20 wt %, the corresponding loss tangent also shown the similar behavior as expected. This revealed the interaction of highly polar and semiconducting PAni with the stable semiconducting Y_2O_3 dispersant. Their synergetic interactions lead to different relaxation phenomena in the system representing a semi crystalline semiconducting system in which charge transport occured *via* electron (polaron) hopping mechanism. This type of trend is in agreement with that reported in the literature.[53] The variations in the dielectric loss as a function of Y_2O_3 content in PAni showed (shown in the inset of Fig. 8) the percolation behavior with a percolation threshold at 20 wt % Y_2O_3 in PAni as observed in case of AC conductivity and dielectric constant studies.

Low Frequency EMI Shielding Effectiveness. The electromagnetic interference shielding effectiveness (EMI SE) of any material is the most important parameter in assessing its efficiency in absorbing and / or attenuating the incident electromagnetic radiations. EMI shielding effectiveness can be expressed as[54]

$$\text{EMI SE} = 10 \log_{10} (P_I/P_T) \text{ dB} \quad (2)$$

Where P_I and P_T are the power (W) of the incident wave and transmitted wave respectively. The capability of shielding is measured in terms of its signal attenuation. The attenuation may also be expressed in terms of the ratio of the magnitudes of the incident electric field (E_I) and transmitted electric field (E_T) by assuming that the fields are plane waves (*i.e.*, EMI SE = 20 $\log_{10}$ E_I/E_T dB). In general, systems that carry electromagnetic waves may be given a simpler description by treating them as networks and focusing only on the exchange of electromagnetic energy at their ports.

EMI SE of PAni-Y_2O_3 composites in the frequency range from 100 Hz to 2 GHz are shown in Figure 9. It was observed that for smaller loading of Y_2O_3 up to a concentration of 20 wt %, the shielding effectiveness (SE) increased. The EMI SE decreases marginally for higher concentration of Y_2O_3 in the PANI matrix following the similar percolation charac-

teristics (with percolation threshold at 20 wt % loading of Y_2O_3 in PAni matrix as shown in inset of Figure 9) as observed in the case of DC electrical conductivity and low frequency transport properties. The shielding effectiveness in these composites decreased marginally with increasing frequencies. It is well known that the EMI SE is proportional to the conductivity as well as permittivity of the material.[55] The distribution of Y_2O_3 in the PAni matrix enhanced the effective interfacial area of the composites. This facilitates high shielding as the composites behaved like a continuous conducting mesh. The reduction in the shielding properties of the composites with the high Y_2O_3 concentration could be explained by the inhomogeneity of the composite to form a continuous network. The crowding effect of Y_2O_3 in the PAni matrix reduced the effectiveness of the composite towards the electromagnetic wave attenuation. But the overall shielding performances of the composites were very effective with the EMI SE values in the range –17.5 dB to –12.5 dB, which is within the purview of practical range. Polyaniline with the stable semiconducting Y_2O_3 contributed appreciably towards increase in the attenuation of electromagnetic radiations.

Conclusions

Incorporation of Y_2O_3 in PAni matrix leads to the formation of composition dependent semiconducting composites with universal frequency dependent AC conductivity obeying the power law. The electrical properties and low frequency EMI shielding characteristics of the composites can be tuned by varying Y_2O_3 loading. The observed dielectric properties of the composites display the prospects of various technological applications of these composites. The variations in the DC conductivity, AC conductivity, dielectric and EMI shielding properties of the composite with varying Y_2O_3 concentration is attributed to the conformational changes in PAni matrix. Due to the effective shielding performance, the composites may also be used for EMI shielding applications in the broad microwave frequency band. A percolation threshold of 20 wt % of Y_2O_3 in PAni matrix as observed in case of various property measurement is a unique feature. We are in a process of preparing these composites in the form of films, as they can be used for practical applications.

Acknowledgments. The Authors would like to thank the management of PES Institute of Technology-Bangalore South Campus, for their support and encouragement towards carrying out this work.

References

1. Chandrasekhar, P. *Conducting Polymers, Fundamentals and Applications: A Practical Approach*; Kluwer Academic: Boston, 1999.
2. Skotheim, T. A.; Elsenbaumer, R. L.; Reynolds, J. R. *Handbook of Conducting Polymers*, 2nd ed.; Dekker, M., Ed.; New York, 1998.
3. Genies, E. M.; Boyle, A.; Lapkowski, M.; Tsintavis, C. *Synth. Met.* **1990**, *36*, 139.
4. Alexander, P.; Ogurtsov, N.; Korzhenko, A.; Shapoval, G. *Prog. Polym. Sci.* **2003**, *28*, 1701.
5. Blinova, N. V.; Stejskal, J.; Trchova, M.; Prokes, J.; Omastova, M. *Eur. Polym. J.* **2007**, *43*, 2331.
6. Gospodinova, N.; Terlemezyan, L. *Prog. Polym. Sci.* **1998**, *23*, 1443.
7. Dey, A.; De, S.; De, A.; De, S. K. *Nanotechnology* **2004**, *15*, 1277.
8. Sung, J. H.; Choi, H. J. *J. Macromol. Sci. B: Phys*. **2005**, *44*, 365.
9. Bae, W. J.; Kim, K. H.; Jo, W. H. *Macromolecules* **2004**, *37*, 9850.
10. Sarkar, A.; Ghosh, P.; Meikap, A. K.; Chattopadhyay, A. K.; Chatterjee, A. K.; Ghosh, M. *J. Phys. D: Appl. Phys.* **2006**, *39*, 3047.
11. Bian, C.; Xue, G. *Mater. Lett.* **2007**, *61*, 1299.
12. Zhang, L.; Wan, M. *J. Phys. Chem. B* **2003**, *107*, 6748.
13. Schnitzler, D. C.; Meruvia, M. S.; Hümmelgen, I. A.; Zarbin, A. J. G. *Chem. Mater.* **2003**, *15*, 4658.
14. Li, X.; Chen, W.; Bian, C.; He, J.; Xu, N.; Xue, G. *Appl. Surf. Sci.* **2003**, *217*, 16.
15. Chuang, F.-Y.;Yang, S.-M. *Synth. Met.* **2005**, *152*, 361.
16. Parvatikar, N.; Jain, S.; Kanamadi, C. M.; Chougule, B. K.; Bhoraskar, S. V.; Ambika Prasad, M. V. N. *J. Appl. Polym. Sci.* **2007**, *103*(2), 653.
17. Makeiff, D. A.; Huber, T. *Synth. Met.* **2006**, *156*, 497.
18. Hatchett, D. W.; Josowicz, M. *Chem. Rev.* **2008**, *108*, 746.
19. Prakash, S.; Kale, B. B.; Amalnerkar, D. P. *Synth. Met.* **1999**, *106*, 53.
20. Sathiyanarayanan, S.; Syed Azim, S.; Venkatachari, G. *Synth. Met.* **2007**, *157*, 205.
21. Gangopadhyay, R.; De, A. *Chem. Mater.* **2000**, *12*, 608.
22. Cochet, M.; Maser, W. K.; Benito, A. M.; CalleJas, M. A.; Martinez, M. T.; Benoit, J. M.; Schreiber, J.; Chauvet, O. *Chem. Commun.* **2001**, *16*, 1450.
23. Dyre, J. C.; Shroder, T. B. *Rev. Mod. Phys.* **2000**, *72*, 873.
24. Wessling, B. *Synth. Met.* **1988**, *27:A*, 83.
25. Singh, K.; Ohlan, A.; Bakshi, A. K.; Dhawan, A. K. *Mater. Chem. Phys.* **2010**, *119*, 201.
26. Saini, D.; Choudhary, V.; Singh, B. P.; Mathur, R. B.; Dhawan, S. K. *Synth. Met.* **2011**, *161*, 1522.
27. Cranton, W. M.; Spink, D. M.; Stevens,V; Thomas, C. B. *Thin Solid Films* **1993**, *226*, 156.
28. Jiayu, D.; Yuan, X.; Pengde, H.; Qitu, Z. *J. Rare earth.* **2010**, *28*, 765.
29. Schubert, D.; Dargusch, R.; Raitano, J.; Chan, S.-W. *Biochem. Biophys. Res. Commun.* **2006**, *342*, 86.
30. Syed Khasim; Raghavendra, S. C.; Revanasiddappa, M.; Sajjan, K. C.; Mohana Lakshmi; Muhammad Faisal. *Bulletin of Materials Science* **2011**, *34*, 1557.
31. Nanni, F.; Travaglia, P.; Valentini, M. *Comp. Sci. Tech.* **2009**, *69*, 485.
32. Pouget, J. P.; Jozefowicz, M. E.; Epstein, A. J.; Tang, X.; MacDiarmid, A. G. *Macromolecules* **1991**, *24*, 779.
33. Du, J.; Liu, Z.; Han, B.; Li, Z.; Zhang, J.; Huang, Y. *Micropor. Mesopor. Mat.* **2005**, *84*, 254.
34. Kang, E. T.; Neoh, K. G.; Tan, K. L. *Prog. Polym. Sci.* **1998**, *23*, 277.
35. Durmus, Z.; Baykal, A.; Kavas, H.; Ozeri, H. S. *Physica B* **2011**, *406*, 1114.
36. Kulkarni, M. V.; Viswanath, A. K.; Marimuthu, R.; Seth, T. *Polym. Eng. Sci.* **2004**, *44*, 1676.
37. Sapurina, I.; Stejskal, J. *Polym Int*. **2008**, *57*, 1295.
38. Anilkumar, K. R.; Parveen, A.; Badiger, G. R.; Ambika Prasad, M. V. N. *Physica B* **2009**, *404*, 1664.
39. Stejskal, J.; Gilbert, R. G. *Pure Appl. Chem.* **2002**, *74*, 857.
40. Zhang, D. *Polym. Test.* **2007**, *26*, 9.
41. Li, X.; Li, X.; Wang, G. *Mater. Chem. Phys*. **2007**, *102*, 140.
42. Long, Y.; Chen, Z.; Shen, J.; Zhang, Z.; Zhang, L.; Huang, K.; Wan, M.; Jin, A.; Gu, C.; Duvail, J. L. *Nanotechnology* **2006**, *17*, 5903.

43. Mott, N. F.; Davis, E. A. *Electronic Processes in Non-crystalline Materials*, Oxford: Clarendon Press; New York: Oxford University Press, 1979.
44. Reghu, M.; Subramanyam, S. V.; Chatterjee, S. *Phys. Rev. B* **1991**, *43*, 4236.
45. Papathanassiou, A. N.; Sakellis, I.; Grammatikakis, J. *Appl. Phys. Lett.* **2007**, *91*, 122911.
46. Bowen, C. R.; Dent, A. C. E.; Almond, D. P.; Comyn, T. P. *Ferroelectrics* **2008**, *370*, 166.
47. Papathanassiou, A. N.; Sakellis, I.; Grammatikakis, J.; Sakkopoulos, S.; Vitoratos, E.; Dalas, E. *Synth. Met.* **2004**, *42*, 81.
48. Hunt, A. G. *Phil. Mag. B* **2001**, *81*, 875.
49. Jiang, J.; Ai, L. H.; Qin, D. B.; Liu, H.; Li, L. C. *Synth. Met*. **2009**, *159*, 695.
50. Kim, H. M.; Lee, C. Y.; Joo, J. *Korean Phys. Soc.* **2000**, *36*, 371.
51. Pinto, N. J.; Shah, P. D.; Kahol, P. K.; McCormic, B. J. *Solid State Commun.* **1996**, *97*, 1029.
52. Baskran, R.; Selvasekarapandian, S.; Hirankumar, G.; Bhuvaneswari, M. S. *J. Power Source* **2004**, *134*, 235.
53. Thomas, P.; Dwarakanath, K.; Varma, K. B. R. *Synth. Met.* **2009**, *159*, 2128.
54. Saini, P.; Choudhary, V. Singh, B. P.; Mathur, R. B.; Dhawan, S. K. *Mater. Chem. Phys.* **2009**, *113*, 919.
55. Pramanik, P. K.; Saha, T. N.; Khastgir, D. *J. Elastomers Plast.* **1991**, *23*, 345.